Hello hello

Håkon Kvernmoen[†]

June 1, 2023

Abstract

Heiie

Contents

1 Introduction

2 Theory

In the following we will always work in atomic units. This entails setting four fundamental constants to the numeric value of 1

$$\hbar = e = m_e = k_e = 1,$$

where $\hbar$ is the reduced Planck constant, e the elementary charge, m_e the electron mass and k_e the Coulomb constant being a factor of 4π multiplied with the permittivity in vacuum. All quantities expressed are understood to be in atomic units, meaning that to convert values to more common sets of units, factors has to be included based on dimensional analysis of the respective quantity. Importantly we note energy, where one atomic unit is equal to $27.2113\ldots$ eV and frequency $4.1341\ldots\cdot10^{16}$ Hz

2.1 Mathematical Framework and Notation

In the following we will use the occupation representation, making use of creation $a_p^\dagger$ and annihilation a_p operators. As a shorthand, we will write $\hat{p}^\dagger \equiv a_p^\dagger$ and $\hat{p} \equiv a_p$ when no confusion can be made. N represents the number of occupied states while L the total number of states in our calculations. The indicies $p, q, \ldots$ are reserved for the L general states, the N occupied states are indexed by $i, j, \ldots$, while the $M \equiv L - N$ unoccupied (virtual) states by $a, b, \ldots$ indicies.

Since we are treating fermionic systems, the canonical anticommutation relations (CAR) are used

$$\{\hat{p}^\dagger, \hat{q}^\dagger\} = \{\hat{p}, \hat{q}\} = 0 \qquad \{\hat{p}^\dagger, \hat{q}\} = \delta_{pq}.$$

One and two body matrix elements are calculated using a computational basis, with explicit expressions for one body Hamiltonians $h(\boldsymbol{x})$ and two body interaction $v(\boldsymbol{x}, \boldsymbol{x}')$ here presented in position space

$$\langle p| \hat{h} |q\rangle = \int d\boldsymbol{x}\, \psi_p^*(x)\hat{h}(\boldsymbol{x})\psi_q(x)$$

$$\langle pq| \hat{v} |rs\rangle = \int d\boldsymbol{x}\, d\boldsymbol{x}'\, \psi_p^*(\boldsymbol{x})\psi_q^*(\boldsymbol{x}')\hat{v}(\boldsymbol{x},\boldsymbol{x}')\psi_r(\boldsymbol{x})\psi_s(\boldsymbol{x}')$$

with ψ_p being a single particle wave function, often chosen to be the eigenfunction of $\hat{h}$. Note that p also contain the spin quantum number, meaning that $d\boldsymbol{x}$ implicitly contains a spin component. If $\hat{h}$ or $\hat{v}$ is spin *independent*, this simply reduces to Kronecker deltas for the spin component. By swapping variables in the integral, we find a symmetry for the two-body matrix elements

$$\langle pq| \hat{v} |rs\rangle = \langle qp| \hat{v} |sr\rangle. \tag{1}$$

It is often convenient to use antisymmetrized matrix elements, defined as

$$\langle pq||rs\rangle = \langle pq| \hat{v} |rs\rangle - \langle pq| \hat{v} |sr\rangle,$$

where the terms are often referred to the *direct* and *exchange* terms respectively. Using the symmetry of Eq. 1, we find an expand symmetry for the antisymmetrized matrix elements

$$\langle pq||rs\rangle = -\langle pq||sr\rangle = -\langle qp||rs\rangle = \langle qp||sr\rangle. \tag{2}$$

The shorthands $h_{pq} \equiv \langle p| \hat{h} |q\rangle$, $v_{rs}^{pq} \equiv \langle pq| \hat{v} |rs\rangle$ and $\bar{v}_{rs}^{pq} \equiv \langle pq||rs\rangle$ will often be used. Using this formulation, a general two-body operator can be constructed

$$\hat{H} = \sum_{pq} h_{pq}\hat{p}^\dagger \hat{q} + \frac{1}{4}\sum_{pqrs} \bar{v}_{rs}^{pq}\hat{p}^\dagger \hat{q}^\dagger \hat{s}\hat{r} \tag{3}$$

The simplest ground state ansatz

$$|\Phi_0\rangle = \hat{i}^\dagger \hat{j}^\dagger \ldots |0\rangle,$$

can be evaluated to calculate the simplest energy estimate using Wicks Theorem [7]

$$\langle \Phi_0| \hat{H} |\Phi_0\rangle = \sum_i h_{ii} + \frac{1}{2}\sum_{ij} \bar{v}_{ij}^{ij} \equiv E_{\text{ref}}, \tag{4}$$

named the *reference energy*. Commonly wicks theorem is applied to Eq. 3 to pick out the Eq. 4 contribution, defining the *normal ordered* Hamiltonian

$$\hat{H} = \hat{H}_{\text{N}} + E_{\text{ref}} = \hat{F}_{\text{N}} + \hat{V}_{\text{N}} + E_{\text{ref}},$$

where $\hat{F}_{\text{N}}$ and $\hat{V}_{\text{N}}$ is the normal ordered *Fock operator* and two body interaction respectively.

$$\hat{F}_{\text{N}} = \sum_{pq} f_{pq}\{\hat{p}^\dagger \hat{q}\}, \tag{5}$$

$$\hat{V}_{\text{N}} = \frac{1}{4}\sum_{pqrs} \bar{v}_{rs}^{pq}\{\hat{p}^\dagger \hat{q}^\dagger \hat{s}\hat{r}\}. \tag{6}$$

The operators inside the curly brackets denotes *normal ordering*. In constructing the Fock operator, the matrix elements f_{pq} are given as

$$f_{pq} = h_{pq} + \sum_i \bar{v}_{qi}^{pi}$$

One major reason for doing this is the applicability of the *Generalized Wicks Theorem* (GWT), such that we only need to consider contractions between different normal ordered strings [4].

$$\hat{H} |\Psi\rangle = E |\Psi\rangle \tag{7}$$

2.2 Hartree-Fock

The Hartree-Fock method is one of the cheapest and most commonly applied many-body methods. Using the reference energy equation Eq. 4, we perform a basis change to the Hartree-Fock basis, based on minimizing the ansatz expectation value. Using Greek letters to index the computational basis $\alpha, \beta \ldots$, going over all states L we can change to the Hartree-Fock basis using

$$|i\rangle = \sum_\alpha C_{\alpha i} |\alpha\rangle$$

where $C_{\alpha i}$ are the basis coefficients. These are the objects used for the parameter search in configuration space. We are however not free to choose an arbitrary transformation, since we require the Hartree-Fock states to be orthogonal $\langle i|j\rangle = \delta_{ij}$. We formulate this constraint as a function of the coefficients C

$$\begin{aligned}
\mathcal{G}(C) &= \sum_{ij} \epsilon_{ij}(\delta_{ij} - \langle i|j\rangle) \\
&= \sum_{ij}\sum_{\alpha\beta} \epsilon_{ij}(\delta_{ij} - C_{\alpha i}^* C_{\beta j} \langle \alpha|\beta\rangle) = 0,
\end{aligned}$$

where ϵ_{ij} as the Lagrange multipliers. The goal is minimizing

$$\begin{aligned}
\mathcal{E}(C) &= \langle \Phi_0| \hat{H} |\Phi_0\rangle = \sum_i \sum_{\alpha\beta} C_{\alpha i}^* C_{\beta i} h_{\alpha\beta} \\
&+ \frac{1}{2}\sum_{ij}\sum_{\alpha\beta\gamma\delta} C_{\alpha i}^* C_{\beta j}^* C_{\gamma i} C_{\delta j} \bar{v}_{\gamma\delta}^{\alpha\beta}
\end{aligned}$$

and thus the relevant Lagrangian then becomes

$$\mathcal{L}(C) = \mathcal{E}(C) + \mathcal{G}(C).$$

The equation to solve are then found by considering a stationary point of the Lagrangian $\delta\mathcal{L} = 0$ wrt. the coefficients C. Performing this minimization, we achieve an

eigenvalue problem with the matrix

$$h_{\alpha\beta}^{\mathrm{HF}} = h_{\alpha\beta} + \sum_{\gamma\delta} \rho_{\gamma\delta} \bar{v}_{\beta\delta}^{\alpha\gamma}, \qquad \rho_{\gamma\delta} = \sum_i C_{\gamma i}^* C_{\delta i} \quad (8)$$

having the coefficients as eigenvectors and the Lagrange multipliers as eigenvalues

$$\sum_{\beta} h_{\alpha\beta}^{\mathrm{HF}} C_{i\beta} = \epsilon_i C_{i\alpha}. \quad (9)$$

Where the Lagrange multipliers are diagonal since by their Hermiticity we can perform a unitary transformation to a basis where they are diagonal $\epsilon = U\epsilon'U^\dagger$. In addition, the matrix $\rho_{\gamma\delta}$ can be interpreted as the density matrix.

2.3 Coupled Cluster

The exact solution $|\Psi\rangle$ is approximated by an exponential ansatz $|\Psi_{\mathrm{CC}}\rangle$

$$|\Psi\rangle \approx |\Psi_{\mathrm{CC}}\rangle \equiv e^{\hat{T}} |\Phi_0\rangle. \quad (10)$$

The operators $\hat{T} = \hat{T}_1 + \hat{T}_2 + \ldots$ acting on the ground state ansatz $|\Phi_0\rangle$ are the so-called *cluster operators* defined as

$$\hat{T}_m = \frac{1}{(m!)^2} \sum_{\substack{ab\ldots \\ ij\ldots}} t_{ij\ldots}^{ab\ldots} \{\hat{a}^\dagger \hat{i} \hat{b}^\dagger \hat{j} \ldots\} \quad (11)$$

where $m \leq N$. The scalars $t_{ij\ldots}^{ab\ldots}$ are unknown expansion coefficients called *amplitudes*, which we need to solve for. All the creation and annihilation operators of Eq. 11 anticommute, giving the restriction that

$$t_{\hat{P}'(ij\ldots)}^{\hat{P}(ab\ldots)} = (-1)^{\sigma(\hat{P}) + \sigma(\hat{P}')} t_{ij\ldots}^{ab\ldots}. \quad (12)$$

Here P and P' permutes $\sigma(P)$ and $\sigma(P')$ indices respectively. This is the reason for the prefactor of Eq. 11, since we have $m!$ ways to independently permute particle and hole indices. Instead of having $(L-N)^m N^m$ independent unknowns, we reduce this number by a factor of $(m!)^2$.

2.4 Doubles Truncation

Considering N cluster operators in the exponential ansatz of Eq. 10 is not computationally feasible for realistic systems. The common practice is to include one or more $\hat{T}_m$ operators, making a truncation on $|\Psi_{\mathrm{CC}}\rangle$ as well. In the following we will include only the double excitation operator $\hat{T}_2$, know as the CCD approximation. This gives us

$$|\Psi\rangle \approx |\Psi_{\mathrm{CC}}\rangle \approx |\Psi_{\mathrm{CCD}}\rangle \equiv e^{\hat{T}_2} |\Phi_0\rangle, \quad (13)$$

$$\hat{T}_2 = \frac{1}{4} \sum_{abij} t_{ij}^{ab} \{\hat{a}^\dagger \hat{i} \hat{b}^\dagger \hat{j}\}, \quad (14)$$

with the four-fold amplitude permutation symmetry following from the CAR [1],

$$t_{ij}^{ab} = -t_{ij}^{ba} = -t_{ji}^{ab} = t_{ji}^{ba}. \quad (15)$$

Incorporating the CCD approximation in the Schrödinger equation (Eq. 7), we see that

$$\hat{H}e^{\hat{T}_2} |\Phi_0\rangle = E e^{\hat{T}_2} |\Phi_0\rangle,$$
$$\hat{H}_{\mathrm{N}} e^{\hat{T}_2} |\Phi_0\rangle = \Delta E_{\mathrm{CCD}} e^{\hat{T}_2} |\Phi_0\rangle, \quad (16)$$

where $\Delta E_{\mathrm{CCD}} = E - E_{\mathrm{ref}}$. Expanding both sides and taking the inner product with $\langle\Phi_0|$, we in principle get an equation for the energy. However, this approach is not amenable to practical computer implementation [2] since the amplitude equation will be coupled with the energy equation. Therefor, we rather apply a similarity transform to Eq. 16 by multiplying by the inverse of $e^{\hat{T}_2}$,

$$e^{-\hat{T}_2} \hat{H}_{\mathrm{N}} e^{-\hat{T}_2} |\Phi_0\rangle = \Delta E_{\mathrm{CCD}} |\Phi_0\rangle$$
$$\overline{H} |\Phi_0\rangle = \Delta E_{\mathrm{CCD}} |\Phi_0\rangle \quad (17)$$

where $\overline{H} = e^{-\hat{T}_2} \hat{H}_{\mathrm{N}} e^{-\hat{T}_2}$ is the similarity transformed Hamiltonian. Using this reformulated eigenvalue problem, we can perform the inner product with different states to calculate both ΔE_{CCD} and t_{ij}^{ab}. Considering $\langle\Phi_0|$ we get

$$\langle\Phi_0| \overline{H} |\Phi_0\rangle = \Delta E_{\mathrm{CCD}}, \quad (18)$$

named the *energy equation*. Considering excited states, we arrive at the *amplitude equations*

$$\langle\Phi_{ij\ldots}^{ab\ldots}| \overline{H} |\Phi_0\rangle, \quad (19)$$

used for finding the unknown amplitudes t_{ij}^{ab}. To find explicit expressions for Eq. 18 and Eq. 19, we expand $\overline{H}$ using the Hausdorff expansion

$$\overline{H} = \hat{H}_{\mathrm{N}} + \left[\hat{H}_{\mathrm{N}}, \hat{T}_2\right] + \frac{1}{2!} \left[\left[\hat{H}_{\mathrm{N}}, \hat{T}_2\right], \hat{T}_2\right]. \quad (20)$$

The truncation at the two-fold commutator comes from the fact that we have a two-body interaction combined with $\hat{T}_2$ only performing double excitations. When evaluated with a doubly excited state, at least one creation or annihilation operator from each of the cluster operators has to be contracted with $\hat{H}_{\mathrm{N}}$. Therefor having eight creation and annihilation operators in two $\hat{T}_2$, four of them can be contracted with the four from $\hat{H}_{\mathrm{N}}$, while the other four with the operators from $\langle\Phi_{ij}^{ab}|$. This gives the CCD amplitude equation calculated from

$$\langle\Phi_{ij}^{ab}| \overline{H} |\Phi_0\rangle = 0 \quad (21)$$

---

[1] For double amplitudes, the index permutation symmetry is equal to that of antisymmetrized two-body matrix elements $\langle pq||rs\rangle$ from Eq. 2.

The calculations can be further simplified from Eq. 20, noting that any creation operator $\hat{a}^\dagger$ or annihilation operator $\hat{i}$ to the left of $\hat{H}_N$ can not give any non-zero contractions due to the lack of a $\hat{a}$ or $\hat{i}^\dagger$ to its left. Therefor we only get contribution from fully contracted $\hat{H}_N$, $\hat{H}_N\hat{T}_2$ and $\hat{H}_N\hat{T}_2\hat{T}_2$ terms, where each $\hat{T}_2$ has at least one leg in $\hat{H}_N$.

To make practical use of Eq. 18 and Eq. 21, a chain of contractions applying the GWT has to be performed. This is a tedious task, thus all amplitude and energy equations here has been calculated using `Drudge` [2]. The energy equation becomes

$$\Delta E_{\text{CCD}} = \frac{1}{4}\sum_{abij}\bar{v}_{ab}^{ij}t_{ij}^{ab}, \tag{22}$$

with the amplitude equation in its pure glory (using Einstein summation convention)

$$
\begin{aligned}
&\bar{v}_{ij}^{ab} + \hat{P}(ab)f_{bc}t_{ij}^{ac} - \hat{P}(ij)f_{kj}t_{ik}^{ab} \\
&+ \frac{1}{2}\bar{v}_{cd}^{ab}t_{ij}^{cd} + \frac{1}{2}\bar{v}_{ij}^{kl}t_{kl}^{ab} + \hat{P}(ab)\hat{P}(ij)\bar{v}_{cj}^{kb}t_{ik}^{ac} \\
&+ \frac{1}{4}\bar{v}_{cd}^{kl}t_{ij}^{cd}t_{kl}^{ab} + \hat{P}(ij)\bar{v}_{cd}^{kl}t_{ik}^{ac}t_{jl}^{bd} \\
&- \frac{1}{2}\hat{P}(ij)\bar{v}_{cd}^{kl}t_{ik}^{dc}t_{lj}^{ab} - \frac{1}{2}\hat{P}(ab)\bar{v}_{cd}^{kl}t_{lk}^{ac}t_{lj}^{db} = 0.
\end{aligned}
\tag{23}
$$

Here we have defined permutation operators $\hat{P}(pq) = 1 - \hat{P}_{pq}$, where $\hat{P}_{pq}$ interchanges the two indices p and q.

3 Method

3.1 Computational Considerations

The methods used to solve both the HF and CCD equations will be outlined in the following section.

3.1.1 Hartree-Fock

Solving Eq. (9) is as stated simply an eigenvalue problem, with ϵ and C as eigenvalues and vectors respectively. However, we see from Eq. 8 that the construction of $h_{\alpha\beta}^{\text{HF}}$ requires the density matrix ρ which again is dependent on the coefficients. To find the correct minimization coefficients an iterative scheme was applied. The initial guess was always chosen to be $C_{ii}^{(0)} = 1$ [3]. As a stopping criterion, the sum of Lagrange multipliers per occupied states between iterations Δ was used. The iterations stop when Δ is below a predetermined tolerance Δ_0. This approach is outlined in Algo. 1.

---

[2]Drudge / Gristmill, Symbolic tensor and non-commutative algebra with powerful automatic code generation and optimization, written by Jinmo Zhao and Gustavo E Scuseria, https://tschijnmo.github.io/drudge/

[3]Note that this is over occupied states only

Algorithm 1 Outline of Hartree-Fock iterative scheme.

$C_{ii}^{(0)} \leftarrow 1$
while $\Delta > \Delta_0$ **do**
$\quad h^{\text{HF}} \leftarrow f(C^{(n-1)})$ Eq. 8
$\quad C^{(n)} \leftarrow \text{Eigenvectors}(h^{\text{HF}})$
$\quad \epsilon^{(n)} \leftarrow \text{Eigenvalues}(h^{\text{HF}})$
$\quad \Delta \leftarrow \sum|\epsilon^{(n)} - \epsilon^{(n-1)}|/N$
end while

3.1.2 Coupled Cluster

The approach for solving the amplitudes in Eq. 21 follow much the same methodology as the HF iterative scheme. Fixed point iterations are a common solution to solving non-linear sets of coupled equations, and is relatively easy to formulate.

Going back to the amplitude equation Eq. 23 we separate the diagonal and off-diagonal part of f_{pq} as f_p^D and f_{pq}^O respectively, giving

$$f_{pq} = \delta_{pq}f_{pp} + (1 - \delta_{pq})f_{pq} = f_p^D + f_{pq}^O.$$

Considering the $\hat{P}(ab)$ term with the Fock matrix

$$\hat{P}(ab)\sum_c f_{bc}t_{ij}^{ac} = \sum_c f_{bc}t_{ij}^{ac} - \sum_c f_{ac}t_{ij}^{bc},$$

we can insert the diagonal and off-diagonal partition of the Fock matrix giving

$$
\begin{aligned}
\sum_c t_{bc}t_{ij}^{ac} &= \sum_c \delta_{bc}f_{bb}t_{ij}^{ac} + (1 - \delta_{bc})f_{bc}t_{ij}^{bc} \\
&= f_b^D t_{ij}^{ab} + \sum_c f_{bc}^O t_{ij}^{ac}
\end{aligned}
$$

Similarly

$$\sum_c f_{ac}t_{ij}^{bc} = -f_a^D t_{ij}^{ab} + \sum_c f_{ac}^O t_{ij}^{bc}$$

Meaning that the $\hat{P}(ab)$ Fock matrix term can be expressed as the sum over the off-diagonal part, in addition to a no-sum $f_a^D + f_b^D$ term.

$$\hat{P}(ab)\sum_c f_{bc}t_{ij}^{ac} = (f_a^D + f_b^D)t_{ij}^{ab} + \hat{P}(ab)\sum_c f_{bc}t_{ij}^{ac}$$

Performing the same decomposition for the $\hat{P}_{ij}$ yields the same decomposition. If we go back to Eq. 23 and call every term except the pure diagonal term $R_{ij}^{ab}(t)$ [4] we get

$$\mathcal{F}_{ij}^{ab}t_{ij}^{ab} + R_{ij}^{ab}(t) = 0,$$

$$t_{ij}^{ab} = -\frac{R_{ij}^{ab}(t)}{\mathcal{F}_{ij}^{ab}},$$

---

[4]Note that this is a function of the amplitudes *resulting* in the four-index term after the sums has been performed.

---

where we have defined

$$\mathcal{F}_{ij}^{ab} = f_a^D + f_b^D - f_i^D - f_j^D.$$

Note that $\mathcal{F}_{ij}^{ab}$ is iteration independent and can be pre-computed. This gives a function suitable for fixed point iterations. It is also possible to calculate the new amplitudes using some percentage of the old amplitudes, *slowly mixing* in the new iterations. Parameterized by the mixing parameter $p \in [0,1)$, we update the amplitudes following

$$t_{ij}^{ab,(n)} = p t_{ij}^{ab,(n-1)} + (1-p)\frac{R_{ij}^{ab}(t^{(n-1)})}{\mathcal{F}_{ij}^{ab}} \qquad (24)$$

Convergence is determined by finding stable solutions to t_{ij}^{ab} thus we evaluate the CCD contribution Eq. 22 each iteration and stop when the difference between iterations is lower than some predetermined tolerance. The procedure is outlined in Algo. 2

Algorithm 2 Outline of CCD iterative scheme.

$t_{ij}^{ab(0)} \leftarrow 0$
while $\Delta > \Delta_0$ **do**
  $t_{ij}^{ab,(n)} \leftarrow p t_{ij}^{ab,(n-1)} + (1-p)\frac{R_{ij}^{ab}(t^{(n-1)})}{\mathcal{F}_{ij}^{ab}}$ Eq. 24
  $E^{(n)} \leftarrow \sum \frac{1}{4}\bar{v}_{ab}^{ij} t_{ij}^{ab,(n-1)}$ Eq. 22
  $\Delta \leftarrow |E^{(n)} - E^{(n-1)}|$
end while

The choice of all zeros for $t^{(0)}$ is somewhat arbitrary, and different choices can be made constrained to the symmetry requirements of Eq. 12. Since we have chosen all zeros, the first iteration will always yield

$$t_{ij}^{ab,(1)} = \frac{\bar{v}_{ij}^{ab}}{\mathcal{F}_{ij}^{ab}}$$

which gives an energy equal to the many-body perturbation theory to the second order (MBPT2)

$$\Delta E_{\text{CCD}}^{(1)} = \sum_{\substack{ab \\ ij}} \frac{|\bar{v}_{ij}^{ab}|^2}{f_a^D + f_b^D - f_i^D - f_j^D} = \Delta E_{\text{MBPT2}}.$$

This displays the perturbative nature of the CC equations. Alternatively one could initialize the amplitudes to give the MBPT2 energy, however due to the miniscule performance enhancements for the systems investigated here, this was not considered necessary.

3.1.3 Numerical efficacy

The iterative amplitude scheme relies heavily on contraction of the rank-4 tensors t_{rs}^{pq} and $\bar{v}_{rs}^{pq}$. Taking the four

contraction term with no permutation from Eq. 23 remembering the summation convention

$$\frac{1}{4}\bar{v}_{cd}^{kl} t_{ij}^{cd} t_{kl}^{ab} \equiv \mathcal{T}_{ij}^{ab}, \qquad (25)$$

we see that we have two sums over the virtual states contributing a factor M^2, while also having a sum over occupied states contributing N^2. Since we create an object $\mathcal{T}_{ij}^{ab}$, these contractions have to be performed for M^2 virtual and N^2 occupied indices, giving this term a total time-complexity of $\mathcal{O}(N^4 M^4)$. Considering a sum over an *intermediate* tensor

$$\chi_{cd}^{ab} = \frac{1}{4} t_{kl}^{ab}\bar{v}_{cd}^{kl},$$

we latch on a time complexity $\mathcal{O}(M^4 N^2)$. By then again contracting with an amplitude, we recover the original contraction from Eq. 25

$$t_{ij}^{cd}\chi_{cd}^{ab} = \frac{1}{4} t_{ij}^{cd} t_{kl}^{ab}\bar{v}_{cd}^{kl}$$

which again has the time complexity $\mathcal{O}(M^4 N^2)$. At the penalty of storing the M^4 elements of χ_{cd}^{ab}, we have reduced the time complexity by a factor of N^2. We could also include more terms in χ_{ij}^{ab} such that more than one term of Eq. 23 can be computed

$$\chi_{ij}^{ab} = \frac{1}{4} t_{kl}^{ab}\bar{v}_{cd}^{kl} + \frac{1}{2}\bar{v}_{cd}^{ab}$$

$$t_{ij}^{cd}\chi_{cd}^{ab} = \frac{1}{4} t_{ij}^{cd} t_{kl}^{ab}\bar{v}_{cd}^{kl} + \frac{1}{2}\bar{v}_{cd}^{ab} t_{ij}^{cd}$$

which will be faster, but not lower the over scaling below $\mathcal{O}(M^4 N^2)$. For the CCD equations, there are no reuse of intermediates and only the summation order yields better time complexities. Through the tensor contraction functionality of `NumPy` [11], optimal paths can be calculated before the summation is performed. Therefor the potential optimizations of this approach was deemed neglectable.

There are however more possibilities for optimization which was not considered here. Based on symmetries of the two-body interaction, only matrix elements which we a priori know will not necessarily be zero can be considered by storing matrix elements and amplitudes in different *symmetry channels*. Additionally, with some index mapping, matrix storage can used allowing for full `BLAS` functionality [3].

3.2 Spin restriction

Both the HF and CCD frameworks presented here treats matrix elements including spin. If the Hamiltonian is spin-independent, both storing and summation over matrix elements can be significantly reduced. Separating relevant quantum numbers and spin, explicitly

$p = (P, \sigma_P)$ with P as relevant numbers and σ_P as spin, we see that a general matrix element

$$\langle pq| \hat{v} |rs\rangle = \langle PQ| \hat{v} |RS\rangle \, \delta_{\sigma_P \sigma_R} \delta_{\sigma_Q \sigma_S},$$

only gives non-zero contributions when both the spins of p, r and q, s align. This reduces the number of matrix elements by a constant factor of 16, improving both storage and computation time. To make use of this however, we must rewrite our equations to use normal matrix elements, instead of antisymmetrized elements.

3.2.1 Hartree-Fock

Taking the reference energy term from the HF Lagrangian, we can explicitly sum out the spin from the one and two body terms. Starting with the diagonal one body term we have

$$\sum_i h_{ii} = \sum_{I \sigma_I} h_{II} \delta_{II} = 2 \sum_I h_{II}.$$

By expanding the antisymmetrized matrix elements, the two body term follows similarly

$$\begin{aligned}
\frac{1}{2} \sum_{ij} \bar{v}_{ij}^{ij} &= \frac{1}{2} \sum_{ij} v_{ij}^{ij} - v_{ji}^{ij} \\
&= \frac{1}{2} \sum_{IJ\sigma_I\sigma_J} v_{IJ}^{IJ}\delta_{\sigma_I\sigma_I}\delta_{\sigma_J\sigma_J} - v_{JI}^{IJ}\delta_{\sigma_I\sigma_J}\delta_{\sigma_I\sigma_J} \\
&= \sum_{IJ} \left(2v_{IJ}^{IJ} - v_{JI}^{IJ}\right).
\end{aligned}$$

The reference energy term Eq. 4 can be expressed with spin summed out as

$$\sum_i h_{ii} + \frac{1}{2} \sum_{ij} \bar{v}_{ij}^{ij} = 2\sum_I h_{II} + \sum_{IJ} \left(2v_{IJ}^{IJ} - v_{JI}^{IJ}\right).$$

Now the same expansion in the computational basis can be performed such as in Sec. 2.2 and by optimizing wrt. to the coefficients C_{AI} with the orthonormality constraint, we get a similar HF matrix

$$h_{AB}^{\text{HF}} = h_{AB} + \sum_{GD} \rho_{GD} v_{BD}^{AG} - \frac{1}{2} \sum_{GD} \rho_{GD} v_{DB}^{AG}$$

where we now have defined the density matrix with a factor two, reflecting the double occupancy of each (spatial) state.

$$\rho_{GD} = 2 \sum_i C_{GI}^* C_{DI}$$

The same iterative scheme from Algo. 1 was used, with the modified HF matrix and energy evaluation.

3.2.2 Coupled Cluster

Motivated by the HF approach, we expand the antisymmetrized matrix elements. Since we additionally have antisymmetric amplitudes, we also expand these. The CCD energy from Eq. 22 then becomes

$$\Delta E_{\text{CCD}} = \frac{1}{4} \sum_{\substack{ab \\ ij}} \bar{v}_{ab}^{ij} t_{ij}^{ab} = \frac{1}{8} \sum_{\substack{ab \\ ij}} (v_{ab}^{ij} - v_{ba}^{ij})(t_{ij}^{ab} - t_{ij}^{ba})$$

We now defined new amplitudes where the antisymmetry is gone, but still the symmetry of the normal two body elements Eq. 1 is present.

$$\tau_{ij}^{ab} = \tau_{ji}^{ba} = \tau_{IJ}^{AB} \delta_{\sigma_A \sigma_I} \delta_{\sigma_B \sigma_J} = \tau_{JI}^{BA} \delta_{\sigma_B \sigma_J} \delta_{\sigma_A \sigma_I} \quad (26)$$

As shown in detail in App. .2, the CCD energy can then be rewritten as

$$\begin{aligned}
\Delta E_{\text{CCD}} &= \frac{1}{2} \sum_{\substack{ab \\ ij}} v_{ab}^{ij}\tau_{ij}^{ab} - v_{ba}^{ij}\tau_{ij}^{ab} \\
&= \sum_{\substack{AB \\ IJ}} \left(2v_{AB}^{IJ} - v_{BA}^{IJ}\right) \tau_{IJ}^{AB}
\end{aligned}$$

Similar approaches can be used to sum the spin out of Eq. 23, which is a drudging and lengthy task. Here the results from [9] is presented. The result has also been calculated using `Drudge`, present in the code base. Einstein summation convention is assumed

$$\begin{aligned}
& v_{IJ}^{AB} + \hat{P}((IA)(JB))\Big[f_{BC}\tau_{IJ}^{AC} - f_{KJ}\tau_{IK}^{AB} \\
& + \frac{1}{2}v_{CD}^{AB}\tau_{IJ}^{CD} + \frac{1}{2}v_{IJ}^{KL}\tau_{KL}^{AB} + 2v_{CJ}^{KB}\tau_{KI}^{AC} \\
& - v_{CJ}^{KB}\tau_{KI}^{AC} - v_{IC}^{KB}\tau_{KJ}^{AC} - v_{JC}^{KB}\tau_{IK}^{AC} \\
& + v_{CD}^{KL}\Big(\frac{1}{2}\tau_{IJ}^{CD}\tau_{KL}^{AB} + 2\tau_{IK}^{AC}\tau_{LJ}^{DB} - 2\tau_{IK}^{AC}\tau_{JL}^{DB} \\
& + \frac{1}{2}\tau_{IK}^{CA}\tau_{LJ}^{BD} - \tau_{IK}^{AD}\tau_{LJ}^{CB} + \tau_{KI}^{AD}\tau_{LJ}^{CB} \\
& + \frac{1}{2}\tau_{IL}^{CB}\tau_{KJ}^{AD} - 2\tau_{KI}^{CD}\tau_{LJ}^{AB} + \tau_{IK}^{CD}\tau_{LJ}^{AB} \\
& - 2\tau_{KL}^{CA}\tau_{IJ}^{DB} + \tau_{KL}^{AC}\tau_{IJ}^{DB}\Big)\Big] = 0
\end{aligned} \quad (27)$$

with

$$\hat{P}((IA)(JB)) = 1 + \hat{P}_{IJ}\hat{P}_{AB}$$

3.3 Quantum Mechanical System

3.3.1 Helium and Beryllium

The initial testing during development of the CCD and RCCD implementations was performed using Hydrogen wave functions. As a choice of basis sets, these functions are 'physically motivated' in the sense of being solutions to the one body electron case. The well-know relevant

quantum numbers determining the form of the spatial wave functions are n as the principal quantum number, with l and m as orbital angular momentum and projection respectively. Due to the spherically symmetric potential, the wave function ψ_{nlm} can be separated in a radial function $R_{nl}(r)$ and a spherical harmonic Y_l^m,

$$\psi_{nlm}(r, \theta, \phi) = R_{nl}(r)Y_l^m(\theta, \phi). \tag{28}$$

The radial part $R_{nl}(r)$ has the form

$$R_{nl}(r) = A_{nl}e^{-r/na_0}\left(\frac{2r}{na_0}\right)^l\left[L_{n-l-1}^{2l+1}(2r/na_0)\right]$$

$$A_{nl} = \sqrt{\left(\frac{2}{na_0}\right)^3 \frac{(n-l-1)!}{2n(n+l)!}}$$

With L as the associated Laguerre polynomials and a_0 the Bohr radius. For $l > 0$ the Coulomb interaction integral of Eq. 28 can not be easily evaluated due to Y_l^m having a non-trivial θ and ϕ dependence. Therefor for simplicity we only consider s orbital ($l = 0$ states), when calculating $\langle pq|\hat{v}|rs\rangle$. This is briefly sketched in App. .1. The one-body term h_{pq} are diagonal with

$$h_{nm} = -\frac{Z}{2n^2}\delta_{nm} \tag{29}$$

We will be interested in calculating the ground state energy for Helium and Beryllium, with two and four electrons respectively. In addition to Hartree-Fock and CCD calculations, a comparison to configuration interaction using singles (CIS) will be performed for both Helium and Beryllium. The results will also be benchmarked against the famous work done by Egil A. Hylleraas [5].

3.3.2 Two-Dimensional Harmonic Oscillator

To test the HF and CCD implementations on larger basis sets, the two-dimensional harmonic oscillator was chosen. N electrons are confined in a potential characterized by the oscillation frequency ω, with a repulsive Coulomb term

$$H = \sum_{i=1}^{N}\left(-\frac{1}{2}\nabla_i^2 + \frac{1}{2}\omega^2 r_i^2\right) + \sum_{i<j}\frac{1}{r_{ij}} \tag{30}$$

where $r_{ij} = |\boldsymbol{r}_i - \boldsymbol{r}_j|$. The natural single particle basis for this problem is the solutions to the non-interactive harmonic oscillator case. Characterized by two quantum numbers n_x and n_y, the position space wave function in Cartesian coordinates are expressed as

$$\psi_{n_x n_y}(x, y) = A_{n_x n_y}H_{n_x}(\sqrt{\omega}x)H_{n_y}(\sqrt{\omega}y)e^{-\omega(x^2+y^2)/2}$$

$$A_{n_x n_y} = \sqrt{\frac{\omega}{\pi 2^{(n_x+n_y)}n_x!n_y!}}$$

The one-body Hamiltonian is diagonal, with the well known energies

$$E_{n_x, n_y} = \hbar\omega(n_x + n_y + 1) \tag{31}$$

for two dimensions. For the Coulomb integral from Eq. 30 a more nuanced consideration is in order. The simplest approach is to solve the Coulomb integrals numerically, however even though we just work in two dimensions, the integral will be two-dimensional with a quite complex integrand. For larger basis sets where $L \sim 100$, this approach can not be performed without any clever performance tricks. Luckily this problem has been solved analytically in spherical coordinates [1], giving a much cheaper way to incorporate the Coulomb integrals. The implementation co-authored by Ø. Schøyen has been used [5].

We will consider closed shell systems, that is the particle number N will always correspond to all sets of (n_x, n_y) which gives the same single particle energy from Eq. 31 and every energy below this. These shell closures are tabulated in Tab. 1.

R	(n_x, n_y)	d	N
1	$(0,0)$	2	2
2	$(1,0)_1$	4	6
3	$(2,0)_1, (1,1)$	6	12
4	$(3,0)_1, (2,1)_1$	8	20
5	$(4,0)_1, (3,1)_1, (2,2)$	10	30
6	$(5,0)_1, (4,1)_1, (3,2)_1$	12	42
7	$(6,0)_1, (5,1)_1, (4,2)_1, (3,3)$	14	56
8	$(7,0)_1, (6,1)_1, (5,2)_1, (4,3)_1$	16	72
9	$(8,0)_1, (7,1)_1, (6,2)_1, (5,3)_1, (4,4)$	18	90

Table 1: Showing shell closure for first 9 shells. Degeneracy follows $d = 2R$ with energy per particle $R\hbar\omega$. The subscript 1 means the set on n can be permuted once, $(x, y)_1 = (x, y), (y, x)$.

The interactive $N = 2$ case for $\omega = 1$ has been solved analytically, giving a ground state energy of 3 a.u.[10]. In addition, [8] have tabulated multiple ω frequencies with up to $N = 20$ electrons, calculated for a variety of CC truncation and schemes.

3.3.3 Doubly Magic Nuclei

Define

$$R \tag{32}$$

---

4 Results

4.1 Helium and Beryllium

The closed shell Helium and Beryllium calculations are presented in Tab. 2, with relative errors compared to FCI in Tab. 3. For both HF add CCD in both restricted and unrestricted schemes, no problems of convergence was encountered. Adding a mixing parameter $p > 0$ for CCD only resulted in slower convergence.

Atom	E_{ref}	CI	FCI	HF	RH
He	-2.7500	-2.8385	-2.9037	-2.8311	-2.83
Be	-13.7160	-14.3621	-14.6674	-14.5083	-14.5

Atom	CCD	RCCD	CCD(HF)	RCCD(HF)
He	-2.7516	-2.7516	-2.8391	-2.8391
Be	-13.7195	-13.7195	-14.5129	-14.5129

Table 2: Ground state energies for Helium and Beryllium in a.u. Calculations done with configuration interaction with both singles and no constraints (full), in addition to HF and CCD in both restricted and unrestricted schemes.

Atom	E_{ref}	CI	HF	RHF
He	5.29	2.25	2.50	2.50
Be	6.49	2.08	1.09	1.09

Atom	CCD	RCCD	CCD(HF)	RCCD(HF)
He	5.24	5.24	2.22	2.22
Be	6.46	6.46	1.05	1.05

Table 3: Relative error in % for Helium and Beryllium from Tab. 2, using the FCI results as the exact energies.

4.2 Harmonic Oscillator

Comparing with the analytical case of two interacting particles at $\omega = 1.0$ having an energy of 3.00, the best results was achieved when using the 12 first shells as basis states. Here HF, CCD with HO basis and CCD with HF basis produced energies off (relative error) 3.161909 (5.397%), 3.089302 (2.977%) and 3.005879 (0.196%) respectively. This gave a clear sign that the basis and algorithm implementations were set up correctly. The results from the restricted and unrestricted schemes were again identical.

A comparison of the elapsed time for each algorithm to converge is presented in Fig. 1. All runs were made using $N = 2$. For $R > 9$, the unrestricted implementation begun slowing down substantially.
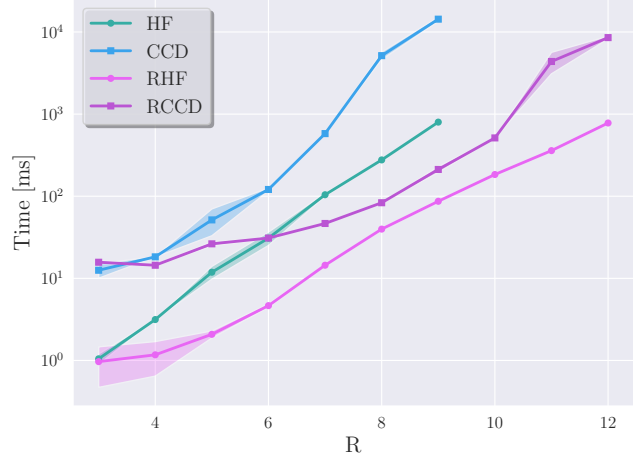

Figure 1: Showing elapsed time in milliseconds, comparing HF and CCD between the unrestricted and restricted schemes. $N = 2$ particles were used, with time being averaged over ten runs. The shaded regions display the standard deviation over the ten runs.

Due to the computational expense when using a large amount of virtual states, all other energy calculations were done in the restricted scheme. Increasing the number of particles in the $\omega = 1.0$ system is presented in Tab. 4. For 12 and 20 particles, convergence for CCD using the HO basis was troublesome. This was in contrast to the HF basis, where no tuning of the mixing parameter was required.

Lowering the frequency to $\omega = 0.5$, we show the same particle systems in Tab. 5. The convergence troubles still stood for the HO basis, but begun for smaller systems with a smaller number of virtual basis states. Here the 20 particle case also required tuning the mixing parameter for the HF basis, with $R > 7$ not achieving convergence with the parameters tested. Lastly lowering the frequency all the way down to $\omega = 0.1$, the 2 and 6 particle systems are presented in Tab. 6. Using 12 and 20 particles did not result in any convergence and are therefor not shown.

R	HF	CCD	CCD(HF)
1	3.253314	3.253314	3.253314
2	3.253314	3.152329	3.152329
3	3.162691	3.141828	3.039049
4	3.162691	3.118684	3.025277
5	3.161921	3.110972	3.017946
6	3.161921	3.103343	3.013924
7	3.161909	3.099330	3.011408
8	3.161909	3.095925	3.009624
9	3.161909	3.093663	3.008351
10	3.161909	3.091818	3.007366
11	3.161909	3.090438	3.006599
12	3.161909	3.089302	3.005979

(a) $N = 2$

R	p	HF	CCD	CCD(HF)
2	N	22.219813	22.219813	22.219813
3	N	21.593198	21.974680	21.423816
4	N	20.766919	21.854198	20.429269
5	N	20.748402	21.793640	20.332466
6	N	20.720257	21.750086	20.274029
7	N	20.720132	21.718843	20.249851
8	N	20.719248	21.695225	20.234708
9	0.30	20.719248	21.675965	20.224387
10	0.30	20.719217	21.661863	20.217073
11	0.30	20.719215	21.649847	20.211538
12	0.30	20.719215	21.640798	20.207259

(b) $N = 6$

R	p	HF	CCD	CCD(HF)
3	>0.99	73.765549	73.765549	73.765549
4	>0.99	70.673849	-	70.324257
5	>0.99	67.569930	-	67.031101
6	>0.99	67.296869	-	66.526674
7	>0.99	66.934745	-	66.049566
8	>0.99	66.923094	-	65.972154
9	>0.99	66.912244	-	65.921206
10	>0.99	66.912035	-	65.889282
11	>0.99	66.911365	-	65.866717
12	>0.99	66.911364	-	65.849773

(c) $N = 12$

R	p	HF	CCD	CCD(HF)
4	>0.99	177.963297	177.963297	177.963297
5	>0.99	168.808284	-	168.459454
6	>0.99	161.339721	-	160.594508
7	>0.99	159.958722	-	158.841116
8	>0.99	158.400172	-	157.038328
9	>0.99	208.177129	-	156.676039
10	>0.99	158.017667	-	156.367932
11	>0.99	158.010276	-	156.292420
12	>0.99	158.004951	-	156.238255

(d) $N = 20$

Table 4: Showing ground state energies for $\omega = 1.0$, when increasing the number of shells R used for the calculation up to and including $R = 12$. The four entries Tab. 4a,Tab. 4b,Tab. 4c and Tab. 4d shows 2, 6, 12 and 20 particles respectively. Restricted schemes have been used for all calculations, with CCD and CCD(HF) using the HO and HF basis respectively. The column p displays the mixing parameter for the HO basis used when convergence without it was not achieved, with 'N' marking no mixing required. A dashed line '-' for the energy marks no convergence across different mixing parameters.

R	HF	CCD	CCD(HF)
1	1.886227	1.886227	1.886227
2	1.886227	1.786915	1.786915
3	1.799856	1.778907	1.681981
4	1.799856	1.760121	1.673883
5	1.799748	1.754389	1.670056
6	1.799748	1.748238	1.667808
7	1.799745	1.745232	1.666479
8	1.799745	1.742551	1.665532
9	1.799743	1.740856	1.664848
10	1.799743	1.739446	1.664278
11	1.799742	1.738412	1.663866
12	1.799742	1.737563	1.663523

(a) $N = 2$

R	p	HF	CCD	CCD(HF)
2	N	13.640713	13.640713	13.640713
3	N	13.051620	13.385995	12.901525
4	N	12.357471	13.261110	12.057347
5	>0.99	12.325128	-	11.935004
6	>0.99	12.271499	-	11.864102
7	>0.99	12.271375	-	11.849764
8	>0.99	12.271361	-	11.841326
9	>0.99	12.271337	-	11.835472
10	>0.99	12.271326	-	11.831348
11	>0.99	12.271324	-	11.828237
12	>0.99	12.271320	-	11.825837

(b) $N = 6$

R	p	HF	CCD	CCD(HF)
3	>0.99	46.361130	46.361130	46.361130
4	>0.99	43.663267	-	43.309862
5	>0.99	41.108851	-	40.654710
6	>0.99	40.750512	-	40.068342
7	>0.99	40.302719	-	39.508497
8	>0.99	40.263752	-	39.399125
9	>0.99	40.216688	-	39.329313
10	>0.99	40.216252	-	39.309411
11	>0.99	40.216195	-	39.296003
12	>0.99	40.216165	-	39.285970

(c) $N = 12$

R	p	$p(HF)$	HF	CCD	CCD(HF)
4	>0.99	N	113.412648	113.412648	113.412648
5	>0.99	0.20	105.227282	-	104.896465
6	>0.99	0.20	99.754600	-	99.119518
7	>0.99	>0.99	131.446882	-	-
8	>0.99	>0.99	133.900840	-	-
9	>0.99	>0.99	134.132319	-	-
10	>0.99	>0.99	133.574242	-	-
11	>0.99	>0.99	133.244135	-	-
12	>0.99	>0.99	133.178089	-	-

(d) $N = 20$

Table 5: Showing ground state energies for $\omega = 0.5$, when increasing the number of shells R used for the calculation up to and including $R = 12$. The four entries Tab. 5a,Tab. 5b,Tab. 5c and Tab. 5d shows 2, 6, 12 and 20 particles respectively. Restricted schemes have been used for all calculations, with CCD and CCD(HF) using the HO and HF basis respectively. The columns p and $p(HO)$ displays the mixing parameter used for the HO and HF basis respectively when convergence without it was not achieved, with 'N' marking no mixing required. A dashed line '-' for the energy marks no convergence across different mixing parameters.

R	p	$p(HF)$	HF	CCD	CCD(HF)
1	N	N	0.596333	0.596333	0.596333
2	N	N	0.596333	0.512521	0.512521
3	N	N	0.526903	0.505981	0.442244
4	N	N	0.526903	0.499233	0.442018
5	0.30	N	0.525666	0.497206	0.443337
6	0.30	N	0.525666	0.494263	0.443147
7	0.30	N	0.525635	0.493172	0.443050
8	0.30	N	0.525635	0.498285	0.442974
9	0.30	N	0.525635	0.491290	0.442921
10	0.30	N	0.525635	0.490676	0.442887
11	0.50	N	0.525635	0.490305	0.442856
12	0.50	0.30	0.525635	0.489960	0.442849

(a) $N = 2$

R	p	$p(HF)$	HF	CCD	CCD(HF)
2	>0.99	N	4.864244	4.864244	4.864244
3	>0.99	N	4.435740	-	4.319916
4	>0.99	N	4.019787	-	3.829968
5	>0.99	N	3.963148	-	3.666723
6	>0.99	N	3.870617	-	3.597876
7	>0.99	0.30	3.863135	-	3.590411
8	>0.99	0.30	3.852880	-	3.587734
9	>0.99	0.30	3.852591	-	3.587314
10	>0.99	0.30	3.852393	-	3.587159
11	>0.99	0.30	3.852391	-	3.586844
12	>0.99	0.30	3.852382	-	3.586606

(b) $N = 6$

Table 6: Showing ground state energies for $\omega = 1.0$, when increasing the number of shells R used for the calculation up to and including $R = 12$. The four entries Tab. 6a and Tab. 6b shows 2 and 6 particles respectively. Restricted schemes have been used for all calculations, with CCD and CCD(HF) using the HO and HF basis respectively. The columns p and $p(HO)$ displays the mixing parameter used for the HO and HF basis respectively when convergence without it was not achieved, with 'N' marking no mixing required. A dashed line '-' for the energy marks no convergence across different mixing parameters.

5 Discussion

5.1 Helium and Beryllium

The Helium and Beryllium calculations were presented in Tab. 2. Comparing with the FCI calculated the values, we see from the relative error Tab. 3 that performing a CCD calculation using either the Hydrogen basis or HF basis improved over the reference energy in each scheme. Comparing CI with HF, we see that CI performed better for Helium while HF actually performing substantially better for Beryllium. CCD using the HF basis did beat both CI and HF in both cases, however the margins were not enormous.

The Hylleraas result [5] was -79.005 eV or -2.903 in atomic units is however much more precise. Inclusion of larger parts of the space, such as considering CISD as CCSD would improve results. Small basis sets such as this could serve as a good benchmarking system going forwards with the more complex solvers.

One could of course also expand the space, including more and more s-orbitals. There is however a quite limiting basis when only $l = 0$ basis states are included. Lifting the $l = 0$ was explored in this work, however difficulties trough angular integrands arose, such as

$$\frac{|Y_{l_1}^{m_1}(\theta_1, \phi_1)|^2 |Y_{l_2}^{m_2}(\theta_2, \phi_2)|^2}{\sqrt{r_1^2 + r_2^2 - 2r_1 r_2 \cos\theta_2}}.$$

Further investigation into integration techniques concerning spherical harmonics would be required. The algebraic solver `SymPy` did require a lot of 'hand holding' in terms of the s-integrals, and presumably this would also be the case when considering less trivial angular integrals. Using one of the many Slater-type orbitals (STOs) or Gaussian-type orbitals (GTOs) is commonly the preferred method in the literature, having closed form recursion relation and being well documented. The problem of $l \neq 0$ integrals might be one of the reasons why Hydrogen-like orbitals are not as prevalent, despite being physically motivated for smaller atoms.

5.2 Performance

Considering the time benchmarking from Fig. 1, it was clear that the restricted implementations were a worthwhile task. For $R > 9$, the unrestricted CCD had a quite large gap in performance. This could be due to the $\mathcal{O}(M^4 N^2)$ scaling from Eq. 25, however another hypothesis is the memory usage. In the naive storage scheme where $\bar{v}_{rs}^{pq}$ needs to store L^4 elements, $R = 10$ would

Better storage schemes such as matrix representations mapping $ij \rightarrow I$ and $ab \rightarrow A$ could increase computational performance, due to better usage of `BLAS` functionality. This was not done however due to the main performance focus being comparing restricted to unrestricted schemes. In future work, a more systemic consideration

of computational complexity would be desirable, pushing the limits on larger basis sets.

5.3 Harmonic Oscillator

Comparing with the analytical result for $\omega = 1.0$ and two particles, the relative error using a HO and HF basis have 2.997% and 0.196% respectively with $R = 12$ basis states. This difference is quite more substantial compared with the Helium and Beryllium results. This indicates that the mean field approximation of the average electron-electron interaction is somewhat representative of the system. On the other hand, a simple HF calculation produced a relative error of 5.397%, meaning that electron-electron correlations also play an important role when one wishes to describe the system more accurately. Comparing with [8], the same potential using $R = 12$ shells as basis states yielded a relative error of 0.0218%. This indicates that the inclusion of singles excitations also plays an important role to achieve high precision results.

5.3.1 Increasing the Number of Particles

From the detailed $\omega = 1.0$ for 2, 6, 12 and 20 particles Tab. 4 the energy per particle increases. For $N = 2$ we have $E/N = 1.502990$, increasing to 3.367877 for $N = 6$ and 5.487481 for $N = 12$, while the $N = 20$ case tops it off with $E/N = 7.811913$. Comparing with the non-interacting solutions of 1.00, 1.67, 2.34 and 3.00, we move from having $\sim 150\%$ of the non-interacting solution for 2 particles to $\sim 260\%$ for 20 particles. It is clear that adding more interactive particles in the trap increases the energy due to electron-electron repulsion.

Convergence using the HO basis was difficult for 12 and 20 particles. This can be explained by the true eigenstates of the interacting system deviating from the HO solution when the interaction plays a larger role. By making linear combinations of HO basis states and accounting for some electron-electron interaction by a mean field approximation, more accurate single particle eigenstates are created and thus convergence was achieved using the HF basis.

5.3.2 Turing the Frequency Down

The $\omega = 0.5$ results from Tab. 5 yielded an energy per particle of 0.831762, 1.970973 and 3.273831 for 2, 6 and 12 particles respectively. Comparing with the non-interacting case for 0.5, we contain $\sim 160\%, \sim 240\%$ and $\sim 280\%$ of the non-interacting solution for 2, 6 and 12 particles. Thus decreasing the frequency makes the electron-electron repulsion play a bigger role than the HO trap. Making the HF basis converge is an easier job than the HO basis for the same reasons as for the $\omega = 1.0$ case, just more prevalent due to the interaction playing a bigger role. Additionally, achieving convergence for 20

particles using the HF basis also presented some problems. There are two reasons for this.

Firstly CC is perturbative in nature, meaning that when the non-interacting single particle energies moves closer and closer (since the frequency decreases), we move towards an almost degenerate state. As seen in Eq. 24, we divide by the diagonal Fock matrix, where the main contribution is the single particle energies. When $\epsilon_a + \epsilon_b - \epsilon_i - \epsilon_j \to 0$, the new amplitude contribution will be inflated. This can be counteracted by turning up the mixing parameter p, but this might yield slow or no convergence of the amplitudes.

Secondly for low frequencies, the electron-electron repulsion be so large that the HO trap is not strong enough to contain the particles, such that we actually have an unbound system. For an unbound system, the HO solutions are not the correct basis states despite showing much of the same sinusoidal behavior as the free particle.

These effects are even more prevalent for the $\omega = 0.1$ system Tab. 6, where convergence was only possible for 2 and 6 particles. Here the system is suspected to be unbound when filling the $R = 3$ shell completely.

Defiantly mention

1. CC not variational bad.

2. HF basis good

3. ~~Hydrogen $l \neq 0$ difficult.~~

4. ~~Lower frequencies harder for convergence.~~

5. ~~Not having singles when comparing to article~~

6. How much does energy improve from ref to HF compared to HF to CCD

6   Concluding remarks

References

[1] E. Anisimovas and A. Matulis. Energy spectra of few-electron quantum dots. *Journal of Physics: Condensed Matter*, 10(3):601, January 1998.

[2] Rodney J. Bartlett, Clifford E. Dykstra, and Josef Paldus. Coupled-Cluster Methods for Molecular Calculations. In Clifford E. Dykstra, editor, *Advanced Theories and Computational Approaches to the Electronic Structure of Molecules*, NATO ASI Series, pages 127–159. Springer Netherlands, Dordrecht, 1984.

[3] L Susan Blackford, Antoine Petitet, Roldan Pozo, Karin Remington, R Clint Whaley, James Demmel, Jack Dongarra, Iain Duff, Sven Hammarling, Greg Henry, et al. An updated set of basic linear algebra subprograms (blas). *ACM Transactions on Mathematical Software*, 28(2):135–151, 2002.

[4] L. Ferialdi and L. Diósi. General Wick's Theorem for bosonic and fermionic operators. *Physical Review A*, 104(5):052209, November 2021. arXiv:2110.02920 [hep-th, physics:math-ph, physics:quant-ph].

[5] Egil A. Hylleraas and Bjarne Undheim. Numerische Berechnung der 2S-Terme von Ortho- und Par-Helium. *Zeitschrift für Physik*, 65(11):759–772, November 1930.

[6] Aaron Meurer, Christopher P. Smith, Mateusz Paprocki, Ondřej Čertík, Sergey B. Kirpichev, Matthew Rocklin, AMiT Kumar, Sergiu Ivanov, Jason K. Moore, Sartaj Singh, Thilina Rathnayake, Sean Vig, Brian E. Granger, Richard P. Muller, Francesco Bonazzi, Harsh Gupta, Shivam Vats, Fredrik Johansson, Fabian Pedregosa, Matthew J. Curry, Andy R. Terrel, Štěpán Roučka, Ashutosh Saboo, Isuru Fernando, Sumith Kulal, Robert Cimrman, and Anthony Scopatz. Sympy: symbolic computing in python. *PeerJ Computer Science*, 3:e103, January 2017.

[7] Luca Guido Molinari. Notes on Wick's theorem in many-body theory, October 2017. arXiv:1710.09248 [cond-mat, physics:math-ph].

[8] M. Pedersen Lohne, G. Hagen, M. Hjorth-Jensen, S. Kvaal, and F. Pederiva. *Ab initio* computation of the energies of circular quantum dots. *Physical Review B*, 84(11):115302, September 2011.

[9] Isaiah Shavitt and Rodney J. Bartlett. *Many-Body Methods in Chemistry and Physics: MBPT and Coupled-Cluster Theory*. Cambridge Molecular Science. Cambridge University Press, 2009.

[10] M. Taut. Two electrons in a homogeneous magnetic field: particular analytical solutions. *Journal of Physics A: Mathematical and General*, 27(3):1045, February 1994.

[11] Stefan Van Der Walt, S. Chris Colbert, and Gaël Varoquaux. The numpy array: a structure for efficient numerical computation. *Computing in Science & Engineering*, 13(2):22–30, March 2011. arXiv:1102.1523 [cs].

7 Appendix

.1 Hydrogen Coulomb integrals

Considering states without orbital angular momentum, we remove the dependence on the two quantum numbers l and m, giving

$$\psi_{nlm}(r,\theta,\phi) \longrightarrow \psi_n(r,\theta,\phi)$$
$$= \sqrt{\left(\frac{4}{n^5}\right)} e^{-r/n} L_{n-1}^1(2r/n) Y_0^0.$$

Where we work in distances of the Bohr radius $r/a_0 \longrightarrow r$. Since the Coulomb integral is over two $\boldsymbol{r}_1, \boldsymbol{r}_2 \in \mathbb{R}^3$ spaces, we align $\boldsymbol{r}_1$ along the y-axis and perform the $\boldsymbol{r}_2$ integral first. In spherical coordinates, the Coulomb interaction then becomes

$$\hat{v}(\boldsymbol{r}_1, \boldsymbol{r}_2) = \frac{Z}{|\boldsymbol{r}_1 - \boldsymbol{r}_2|} = \frac{Z}{\sqrt{r_1^2 + r_2^2 - 2r_1 r_2 \cos\theta_2}} \quad (.1)$$

With these preparations, the integrals can be solved for all p, q, r, s combinations. The integrals were solved using `SymPy` [6]

.2 Detailed Spin Restricted Coupled Cluster Energy

We begin by expanding the antisymmetrized terms in the CCD energy expression from Eq. 22

$$\Delta E_{\mathrm{CCD}} = \frac{1}{4} \sum_{\substack{ab \\ ij}} \bar{v}_{ab}^{ij} t_{ij}^{ab} = \frac{1}{8} \sum_{\substack{ab \\ ij}} (v_{ab}^{ij} - v_{ba}^{ij})(t_{ij}^{ab} - t_{ij}^{ba})$$

The restricted amplitudes are related to the unrestricted by

$$t_{ij}^{ab} = \tau_{ij}^{ab} - \tau_{ij}^{ba}$$

Meaning that

$$t_{ij}^{ab} - t_{ij}^{ba} = \left(\tau_{ij}^{ab} - \tau_{ij}^{ba}\right) - \left(\tau_{ij}^{ba} - \tau_{ij}^{ab}\right)$$
$$= 2\left(\tau_{ij}^{ab} - \tau_{ij}^{ba}\right)$$

we insert the restricted amplitudes and expand

$$\Delta E_{\mathrm{CCD}} = \frac{1}{4} \sum_{\substack{ab \\ ij}} (v_{ab}^{ij} - v_{ba}^{ij})(\tau_{ij}^{ab} - \tau_{ij}^{ba})$$
$$= \frac{1}{4} \sum_{\substack{ab \\ ij}} v_{ab}^{ij}\tau_{ij}^{ab} + \underbrace{v_{ba}^{ij}\tau_{ij}^{ba}}_{C_1} - v_{ba}^{ij}\tau_{ij}^{ab} - \underbrace{v_{ab}^{ij}\tau_{ij}^{ba}}_{C_2}.$$

Then by application of the matrix element Eq. 1 and amplitude Eq. 26 symmetries, we see from the terms C_1

and C_2,

$$C_1 = \sum_{\substack{ab \\ ij}} v_{ba}^{ij}\tau_{ij}^{ba} = \sum_{\substack{ab \\ ij}} v_{ba}^{ij}\tau_{ji}^{ab} = \sum_{\substack{ab \\ ij}} v_{ab}^{ji}\tau_{ji}^{ab} = \sum_{\substack{ab \\ ij}} v_{ab}^{ij}\tau_{ij}^{ab}$$

$$C_2 = \sum_{\substack{ab \\ ij}} v_{ab}^{ij}\tau_{ij}^{ba} = \sum_{\substack{ab \\ ij}} v_{ba}^{ji}\tau_{ji}^{ab} = \sum_{\substack{ab \\ ij}} v_{ba}^{ij}\tau_{ij}^{ab}$$

Inserting back into ΔE_{CCD} we find

$$\Delta E_{\mathrm{CCD}} = \frac{1}{2} \sum_{\substack{ab \\ ij}} v_{ab}^{ij}\tau_{ij}^{ab} - v_{ba}^{ij}\tau_{ab}^{ij}$$

Now we explicitly sum over the spins $\{\sigma_A, \sigma_B, \sigma_I, \sigma_J\}$ giving

$$\sum_{\substack{ab \\ ij}} v_{ab}^{ij}\tau_{ij}^{ab} = \sum_{\substack{AB \\ IJ}} \sum_{\substack{\sigma_A\sigma_B \\ \sigma_I\sigma_J}} v_{AB}^{IJ}\tau_{IJ}^{AB} \delta_{\sigma_A\sigma_I}\delta_{\sigma_B\sigma_J}$$
$$= \sum_{\substack{AB \\ IJ}} \sum_{\sigma_A\sigma_B} v_{AB}^{IJ}\tau_{IJ}^{AB} = 4\sum_{\substack{AB \\ IJ}} v_{AB}^{IJ}\tau_{IJ}^{AB}$$

$$\sum_{\substack{ab \\ ij}} v_{ba}^{ij}\tau_{ij}^{ab} = \sum_{\substack{AB \\ IJ}} \sum_{\substack{\sigma_A\sigma_B \\ \sigma_I\sigma_J}} v_{BA}^{IJ}\tau_{IJ}^{AB} \delta_{\sigma_B\sigma_I}\delta_{\sigma_A\sigma_J}\delta_{\sigma_A\sigma_I}\delta_{\sigma_B\sigma_J}$$
$$= \sum_{\substack{AB \\ IJ}} \sum_{\sigma_A\sigma_B} v_{BA}^{IJ}\tau_{IJ}^{AB} \delta_{\sigma_A\sigma_B}$$
$$= 2\sum_{\substack{AB \\ IJ}} v_{BA}^{IJ}\tau_{IJ}^{AB}$$

Giving the total energy expression after spin has been summed out

$$\Delta E_{\mathrm{CCD}} = \frac{1}{2} \sum_{\substack{ab \\ ij}} v_{ab}^{ij}\tau_{ij}^{ab} - v_{ba}^{ij}\tau_{ij}^{ab}$$
$$= \sum_{\substack{AB \\ IJ}} \left(2v_{AB}^{IJ} - v_{BA}^{IJ}\right) \tau_{IJ}^{AB}$$